

## Research Article

# Statistical and Experimental Investigation of Hardened AISI H11 Steel in CNC Turning with Alternative Measurement Methods

Emrah Şahin <sup>1</sup> and İsmail Esen <sup>2</sup>

<sup>1</sup>Department of Electricity and Energy, Vocational College, Çankırı Karatekin University, Çankırı 18200, Turkey

<sup>2</sup>Department of Mechanical Engineering, Faculty of Engineering, Karabük University, Karabük 78050, Turkey

Correspondence should be addressed to Emrah Şahin; [emrah.sahin@karatekin.edu.tr](mailto:emrah.sahin@karatekin.edu.tr)

Received 30 May 2021; Revised 27 August 2021; Accepted 30 August 2021; Published 23 September 2021

Academic Editor: Tomasz Trzepieciński

Copyright © 2021 Emrah Şahin and İsmail Esen. This is an open access article distributed under the Creative Commons Attribution License, which permits unrestricted use, distribution, and reproduction in any medium, provided the original work is properly cited.

In recent years, hard turning, an alternative to grinding, which provides low cost and good surface quality, has become an attractive method to the manufacturers. In this experimental study, AISI H11 hot work tool steel that has been hardened up to 50 HRC was subjected to hard turning tests with coated carbide tooling. The analyses were carried out by applying response surface methodology with the analysis of variance method. A total of 27 experiments were modeled utilizing  $3^3$  full factorial design and were carried out using a CNC lathe. The effects of the cutting parameters on surface roughness, energy consumption, electric current value, and sound intensity level were investigated. Optimum cutting parameters and levels were determined according to these optimum values. The relationship between cutting parameters and output variables was analyzed with two-dimensional and three-dimensional graphics. The results show that while the most effective parameter on the surface roughness was the feed rate (88.62%), the most effective parameter on the sound intensity level was the cutting speed (44.92%). In addition, the cutting depth was the most effective parameter on both electric current (52.20%) and energy consumption (46.15%). Finally, regression coefficients were determined as a mathematical model, and it was observed that this estimated model gave results that were very similar to those achieved with real experiment (correlation values: 97.64% for surface roughness, 98.72% for energy consumption, 97.22% for electric current value, and 91.38% for sound intensity level).

## 1. Introduction

Hard turning has been an important research topic in recent years. Hard turning is the phenomenon of machining at very high cutting speeds. It is an exceedingly difficult and delicate procedure [1]. In the hard turning process, grinding quality or a better surface quality is obtained without grinding [2]. This situation provides advantages in terms of money and time [3]. AISI H11 is a widely used chromium hot work tool steel and has a place of importance in hard turning due to its rigidity and durability. This material can reach a hardness of 45–55 HRC after heat treatment [4]. Heat treatment improves not only the strength property of the material but also its surface quality in the hard turning process.

In order to complete the finishing turning process with high precision, high machine tool rigidity as well as high and

constant surface speed must be provided on the lathe. Otherwise, the negative effects of friction caused by temperature and wear increase the surface roughness. The effects of friction can be reduced with a good surface quality [5].

In terms of hard turning, researchers have worked on different workpieces with different tools, defined various parameters, and sought solutions to optimize surface quality [6, 7]. The effort to improve surface quality has helped to maximize environmental protection and saved money, energy, and time.

Agrawal et al. [8] studied the effects of surface roughness using an AISI 4340 steel CBN tool with different cutting parameters. According to their results, the most effective parameter in surface roughness is the feed rate followed by cutting speed and depth of cut. In another study, Günay and Yücel [9] machined high alloy white cast iron (Ni) with two

different hardness values (50 and 62 HRC) using ceramic and CBN tools. For both hardness values, they obtained the best surface quality with the CBN tool. In their analysis, they stated that although the most effective parameter is feed rate at 62 HRC hardness, the most effective parameter is cutting speed at 50 HRC hardness.

Studies in the literature show that when processing hardened materials, CBN and ceramic tools are preferred as tool materials due to their high hardness properties [10, 11]. However, these tools are quite expensive and their impact resistance is low. Carbide inserts are 20 times cheaper than CBN [12]. According to literature, carbide tips with 45–55 HRC hardness values give particularly good results [13, 14]. Tiwari et al. [15] processed 52–54 HRC hard material with carbide inserts and achieved good results. Thus, carbide inserts produced to process hard materials can be used in rigid machine tools. For this purpose, the aim is more economical production. Alok and Das [16] machined AISI 52100 with a coated carbide tool. They examined tool wear, surface roughness, and cutting force at different cutting parameters and found cutting speed to be the most effective parameter. Sahu and Choudhury [17] machined AISI 4340 steel with uncoated and TiN-coated carbide inserts. In their experiments, they obtained the best surface quality with a coated carbide tool at high speeds and low feed rates. Aoucci et al. [18] studied the effects of AISI H11 hot work tool steel on surface roughness with three different inserts (CC670, CC650, and CBN7020) at different cutting parameters. They achieved the best surface quality at low feed rates and high cutting speeds and found that the most effective cutting parameter on surface roughness was feed rate.

Recent additions to the literature have shown that a wide nose radius provides better results and is more advantageous for surface roughness [19–21]. Nouioua et al. [22] conducted experiments with three different nose radii. They stated that wide nose radius ( $r$ ) gives low surface roughness value. In contrast, Umamaheswarrao et al. [23], who also concluded that nose radius is the most effective cutting parameter, experimented with three different nose radii (0.4, 0.8, and 1.2) and determined that a nose radius of 0.8 provided optimum results. Panda et al. [24] stated in their study that the most effective parameter on the surface roughness was the nose radius ( $r$ ). In addition, studies showed that surface roughness also depends on the minimum uncut chip thickness (MUCT), especially for low feed rate (less than 0.05), provided that  $r$  (nose radius) < 1 mm [25, 26].

Recent research has also provided important information about the cutting conditions of sound during processing [27]. Sound intensity level used as a practical measurement element by experienced operators is an alternative measurement element for a better understanding of the chip removal process. Şahinnoğlu and Rafighi [28] and Çakır [29] studied sound intensity as well as surface roughness. In both studies, it was determined that the cutting speed and depth of cut were the most effective parameters for the sound intensity level. In addition, sound intensity level measurements were an important measurement method in determining the exposure of employees to loud noise.

Rastorguev and Sevastyanov [30] showed in their study that we can have an idea about the cutting forces by looking at the electric current drawn by the lathe. Measuring electric current has become an alternative measurement method instead of performing a difficult task such as cutting force [29].

One indispensable aspect of manufacturing is that developing technology and increasing populations inevitably lead to increased production and decreased energy resources, which in turn causes energy issues as it is estimated that global energy resources have a reserve of 50 years. Thus, energy must be used efficiently. Choosing appropriate cutting parameters is an important factor in efficient energy use. In other words, by changing cutting parameters and values, energy consumption levels can be improved by looking at the power consumed by the machine and the current values it draws [3, 31, 32]. Negrete and Nájere [33] processed AISI 1045 steel under dry processing conditions and investigated the energy consumption, processing time, material removal rate, specific energy, and surface roughness values in different cutting parameters. They reached the optimum cutting parameters for minimum energy usage in turning operations. Velchev et al. [34] stated that the most effective parameters in the energy consumption model they presented are feed rate and depth of cut.

Optimization has gained great importance in the manufacturing industry. By using ANOVA and RSM, analyses can be made in all areas of production [35–37]. For the hard turning process, various optimization methods (RSM, Taguchi, artificial neural networks, genetic algorithm, and particle swarm optimization) were used by researchers [38–40].

In this experimental study, hardened AISI H11 hot work tool steel was machined on a CNC lathe. A PVD-coated carbide tool with 0.8 mm nose radius was used in the experiments. The aim of this study is to determine and interpret the effects between input and output parameters during the processing of hard material.

Hard turning, which eliminates cylindrical grinding processes, can be used in all areas where hard material is needed in recent years.

The studies on machining so far have focused only on the studies on surface roughness, wear, and cutting forces. The part produced for the machine manufacturer should be smooth, and the sound intensity level should be important. Since determining tool wear is a laborious process, we can have an idea about wear by measuring the sound intensity level. At the same time, the sound intensity level that occurs while the workpiece is being processed is an issue that should be considered especially in terms of occupational health and safety. Employees in the manufacturing industry are exposed to high noise intensity. Therefore, the issue of sound intensity, which is missing in the literature, has become the necessity of the age. Since electric current value measurement is instantaneously measured, it has become a practical measurement method by estimating tool wear and surface roughness values that cannot be measured instantly. Likewise, energy consumption is very important for manufacturers. In other words, its contributions to global warming

(environment) aside from the economic machining show that it is a very important issue. With the information obtained from such studies, it will be possible for manufacturers to reduce their costs and increase their competitive power with high-strength machine parts. Such studies should be accelerated for a sustainable and healthy life in the future. Considering these aspects, a significant contribution has been made to the literature.

## 2. Materials and Methods

The AISI H11 material chosen for this research was one with a diameter of 44 mm and a length of 250 mm. The chemical composition of AISI H11 hot work tool steel is given in Table 1 and its mechanical properties are given in Table 2.

The tailstock was drilled before the material was hardened. The workpiece material was allowed to stand at 950°C for 2 hours and was then suddenly cooled in oil. By applying the vacuum hardening technique, homogeneity in heat treatment was provided. Tempering at 6000°C was done to get the tension of the material. Then tests were conducted to check whether the desired properties were acquired or not. A hardness value of 50 HRC was achieved.

Developments in materials and heat treatment technology have created the issue of machinability. Machinability of a given material is one of the most important problems after obtaining high mechanical strength as these types of materials need to be processed on high-rigidity machines. Therefore, a TTC 630 model CNC lathe manufactured by TAKSAN was used in this experimental study. This machine has 20 kW of power and a maximum speed of 4000 rpm and does not lose precision at high cutting speeds.

Full factorial test design was used for the test material, AISI H11 hot work tool steel. The cutting parameter levels and values for the experiments were presented in Table 3. When determining the cutting parameters for hard turning, the data in the literature and the tool catalogue values were taken into account. As the cutting parameters, 3 different cutting speeds (140, 160, and 180), 3 different feed rates (0.05, 0.09, and 0.13), and 3 different depths of cutting (0.05, 0.10, and 0.15) were used. A total of 27 experiments were modeled utilizing 3<sup>3</sup> full factorial design.

The workpiece material chosen for this research is 44 mm in diameter and 250 mm in length. As shown in Figure 1, the material was connected between tailstock and chuck. Some sawdust was removed from the surface and it was then prepared for the processing experiments. Experiments were repeated 3 times to confirm the reproducibility of the experimental results. 9 experiments were performed on a workpiece material.

A PVD (physical vapor deposition) AlTiN-coated carbide tool with DCMT 11T308 geometry manufactured by TaeguTec was used for the turning of hard materials. New cutting tool was used for each experiment. Coolant was used in the cutting process. Experimental work was done with the mixture obtained by mixing 1/20 boron oil with water. The tool holder was used with a docking angle of 95 degrees and an insert angle of -6 degrees. The tool holder was connected at a distance of 10 mm to reduce vibration.

TABLE 1: Chemical composition of grade AISI H11 steel [41].

Chemical composition	C	Si	Cr	Mo	V	Mn
Content (%)	0.35	1.10	5.10	1.20	0.30	0.40

TABLE 2: Mechanical properties of AISI H11 steel [41].

Yield strength (MPa)	Density (g/cm <sup>3</sup> )	Hardness (HRC)
1620	7.80	50

TABLE 3: Cutting parameters and their levels used in the experiment.

Cutting parameter	Symbol	Units	Level		
			1	2	3
Cutting speed	$V_c$	m/min	140	160	180
Feed rate	$f$	mm/rev	0.05	0.09	0.13
Depth of cut	$a_p$	mm	0.05	0.10	0.15



FIGURE 1: PVD carbide tool 2D representation.

The machines and devices used in the experiment are shown in Figure 2. Immediately after the machining test, the surface roughness value was measured with the Mitutoyo SJ 201 roughness tester. Measurements were taken at 3 different points and the average surface roughness value (Ra) was calculated. The sampling range was selected as 0.8.

The electric current value and sound intensity levels during processing were recorded instantaneously. At the time of processing, a UNIT 201 clamp meter. was used to measure electric current values. Phase values were measured, and voltage values were taken from the regulator. The regulator to which the machine was connected prevents fluctuations in voltage values and changes caused by energy losses from affecting the measurement results.

Sound intensity levels were measured with a Lutron SL 401 sound intensity meter in the Filter A position. Sound intensity measurements were collected when the test environment was quiet.

Energy consumption was calculated using Equation (10) by calculating instantaneous power consumption and total processing times.

The data were analyzed using the Minitab 18 statistics package program. As shown in Figure 3, analysis of variance

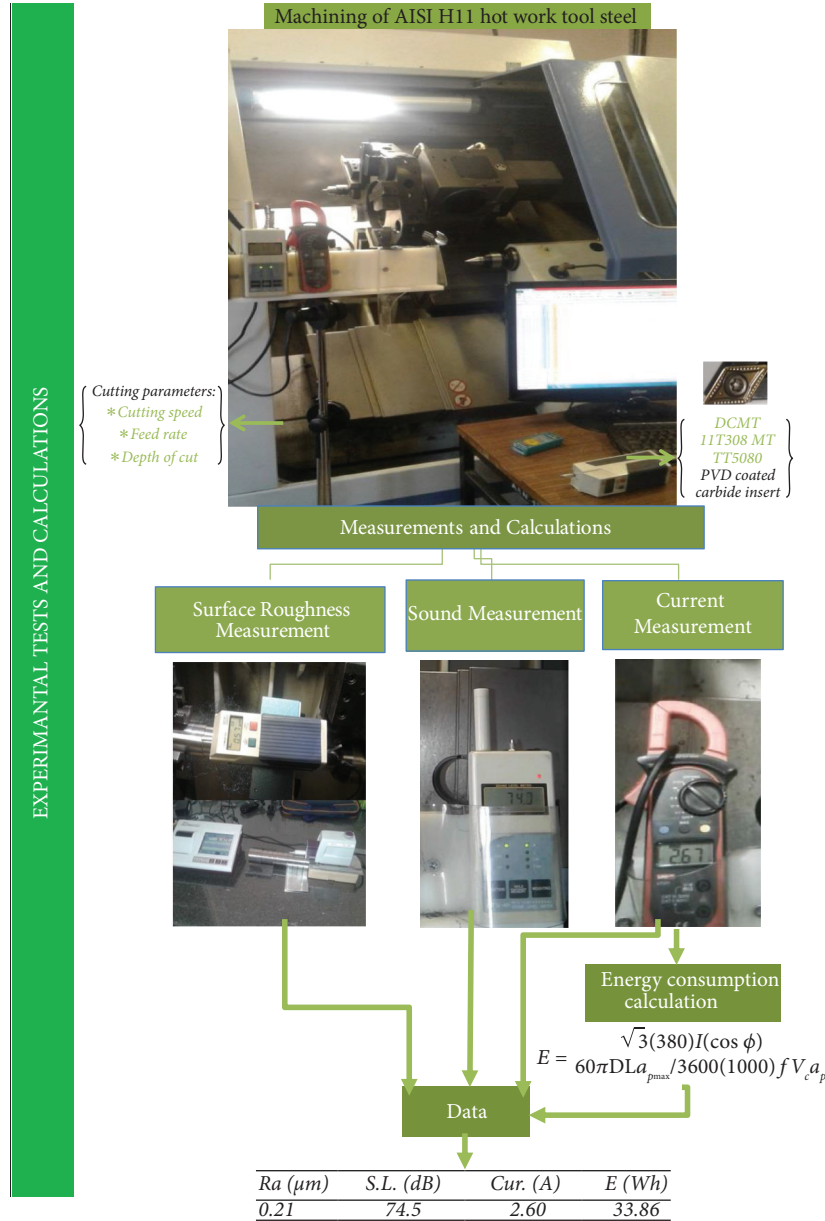


FIGURE 2: Experimental setup.

(ANOVA) modeling and optimization were constructed, respectively. Then, the actual experimental results were compared with the estimated values generated from the mathematical models.

Response surface methodology (RSM) was used to analyze and model the relationship between cutting parameters and response variables. Thanks to RSM, multiple optimizations can be made, and linear, square, and interactive parameters can be specified [40].

$$Y = \varnothing(a_p, V_c, f). \quad (1)$$

The response formula depending on the independent variables is given in equation (1), where  $Y$  is response parameter (energy consumption, current,  $R_a$ , and sound),

$a_p$ ,  $V_c$ , and  $f$  are independent design variables, and  $\varnothing$  is the output parameter function.

### 3. Results and Discussion

The average surface roughness ( $R_a$ ) calculation is given in equation (2) theoretically. We see from this equation that  $R_a$  is directly proportional to the feed rate ( $f$ ) and inversely proportional to the nose radius ( $r$ ). That is, the surface quality deteriorates with increasing feed rate, while the surface quality improves with increasing nose radius. Literature studies support this result [19–21].

$$R_a = \frac{f^2}{32r}. \quad (2)$$

TABLE 4: Energy consumption calculation results of the whole experiment design.

Experiment no.	Depth of cut (mm)	Cutting speed (m/min)	Feed rate (mm/rev)	Surface roughness ( $\mu\text{m}$ )	Sound intensity level (dB)	Electric current (A)	Energy consumption (Wh)
1	0.05	140	0.05	0.21	74.5	2.60	33.86
2	0.05	140	0.09	0.37	74.8	2.64	19.10
3	0.05	140	0.13	0.76	75.0	2.66	13.32
4	0.05	160	0.05	0.22	74.9	2.55	29.06
5	0.05	160	0.09	0.33	75.0	2.60	16.46
6	0.05	160	0.13	0.75	74.9	2.64	11.57
7	0.05	180	0.05	0.18	75.0	2.63	26.64
8	0.05	180	0.09	0.32	75.1	2.67	15.02
9	0.05	180	0.13	0.76	75.3	2.75	10.71
10	0.10	140	0.05	0.23	74.6	2.62	17.06
11	0.10	140	0.09	0.41	74.7	2.68	9.69
12	0.10	140	0.13	0.61	74.8	2.72	6.81
13	0.10	160	0.05	0.22	74.9	2.61	14.87
14	0.10	160	0.09	0.33	75.1	2.68	8.48
15	0.10	160	0.13	0.54	75.2	2.80	6.14
16	0.10	180	0.05	0.18	75.1	2.72	13.77
17	0.10	180	0.09	0.30	75.3	2.78	7.82
18	0.10	180	0.13	0.65	75.5	2.82	5.49
19	0.15	140	0.05	0.16	75.0	2.73	11.85
20	0.15	140	0.09	0.22	75.1	2.78	6.70
21	0.15	140	0.13	0.67	75.3	2.84	4.74
22	0.15	160	0.05	0.18	75.0	2.71	10.29
23	0.15	160	0.09	0.32	75.2	2.85	6.01
24	0.15	160	0.13	0.64	75.3	2.96	4.32
25	0.15	180	0.05	0.17	75.4	2.81	9.49
26	0.15	180	0.09	0.31	75.6	2.93	5.50
27	0.15	180	0.13	0.60	75.8	3.10	4.03

According to the literature studies, the cutting pressure (cutting force) decreased with the increase of the cutting speed and a good quality surface was obtained [21, 42]. When we look at the studies in the literature on hard turning, it shows that the cutting speed is insignificant on the surface roughness [28, 29, 38]. They also stated that the surface quality decreases with increasing cutting speeds [19]. On the contrary, it is known that increasing the depth of cut increases the surface roughness. However, most studies in the literature showed that the depth of cut is unimportant for hard turning [38, 43]. In fact, in some studies, it was observed that the surface roughness decreases slightly at high depths of cut [28, 43]. The rigidity of the machine has also been an important factor in the precision and accuracy of the results.

Sound intensity level measurement and electric current measurement have been alternative measurement methods for predicting tool wear. The electrical current rating of the machine is an indicator of power consumption. Therefore, it will be of great benefit to interpret the selected cutting parameters and electrical current values [29].

The energy consumption is not only related to the instantaneous electric current of the machine but also related to the processing time. Energy consumption is calculated from equation (10) for equal depth of cut [35].

**3.1. Experimental Results.** A total of 27 experiments were modeled utilizing  $3^3$  full factorial design and these tests were

carried out using a CNC lathe. The results of the experiment carried out under wet cutting conditions with coated carbide inserts are given in Table 4.

**3.2. Energy Consumption Calculation Results.** Energy consumption is a function of instantaneous power consumption and total processing time. It is possible to calculate energy consumption using equations (3)–(10).

Instant power consumption is obtained from voltage and current values:

$$P = \sqrt{3}VI \cos \phi, \quad (3)$$

where  $P$  is the instantaneous power consumption,  $V$  is the voltage,  $I$  is the current,  $\phi$  is phase angle, and  $\cos \phi$  is the power factor of the device.

$$P = \sqrt{3}(380)I \cos \phi. \quad (4)$$

The instantaneous power consumption is multiplied by the total processing time and divided by 3600 to obtain energy consumption in kWh.

$$E = \frac{PT}{3600}, \quad (5)$$

where  $E$  is energy consumption and  $T$  is the total processing time.

Spindle speed ( $N$ ) is divided by cutting speed ( $V_c$ ) into the environment:

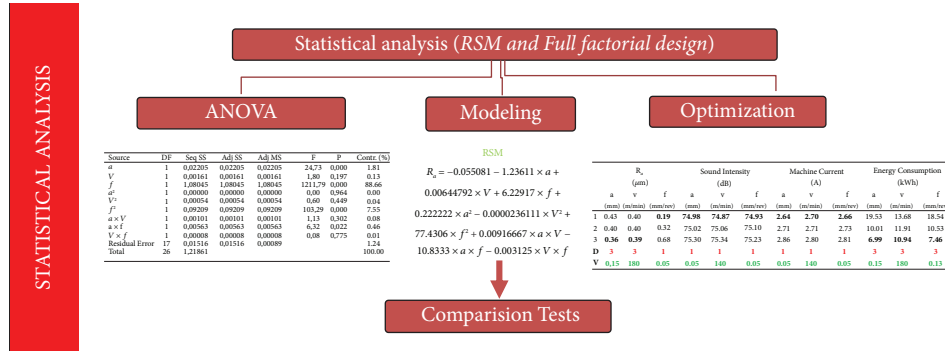


FIGURE 3: Statistical analysis.

$$N = \frac{1000V_c}{\pi D} \quad (6)$$

Machining time ( $t$ ) is obtained by dividing the machining length ( $L$ ) of the workpiece material by the feed rate ( $f$ ) and the spindle speed ( $N$ ):

$$t = \frac{60L}{fN} \quad (7)$$

Machining time when equation (7) is substituted in equation (6) is

$$t = \frac{60\pi DL}{1000fV_c} \quad (8)$$

Total machining time ( $T$ ) is obtained by taking into account the depth of cut ( $a_p$ ):

$$T = \frac{60\pi DL a_{pmax}}{1000fV_c a_p} \quad (9)$$

If the instantaneous power consumption ( $P$ ) and total processing time ( $T$ ) are used in equation (5), the energy consumption ( $E$ ) is

$$E = \frac{\sqrt{3}(380)I(\cos \phi)60\pi DL a_{pmax}}{3600(1000)fV_c a_p} \quad (10)$$

From equation (10), energy consumption was calculated for each experiment and is expressed in Table 4.

**3.3. Statistical Analysis.** The experimental data was analyzed using the Minitab 18 statistics package and the results were interpreted through statistical analysis. The analyses were carried out by applying response surface methodology (RSM) with the analysis of variance (ANOVA) method. These analyses were carried out for a 95% confidence level ( $\alpha = 0.05$  significance level).

Statistical analysis is summarized in Figure 2. Effect rates were determined by ANOVA and mathematical models were created, respectively. The best surface quality, lowest energy consumption, lowest sound intensity level, and lowest electric current values were selected for each cutting parameter. Optimum cutting parameters and levels were determined according to these optimum values. The relationship between cutting parameters and output variables was analyzed with two-dimensional and three-dimensional graphics. Finally, the

actual experiment results were compared with the estimated values created from the mathematical models.

**3.3.1. Main Effect Plots.** Table 5 shows the main effect graphs for each response parameter. The optimum level of input values is indicated in red. Surface roughness ( $R_a$ ), sound intensity level, and electric current values increased with increasing feed rates. On the contrary, energy consumption decreased with increasing feed rates. In addition, as the depth of cut and cutting speed increased, the sound intensity level and electric current values increased. On the other hand, as these values increased, the energy consumption values decreased. As the depth of cut increased, the surface roughness decreased slightly. As the cutting speed values increased, there was a limited decrease in the surface roughness.

**3.3.2. Analysis of Variance (ANOVA).** F, P, and DF values in the ANOVA tables are variance ratio, significant factor, and degrees of freedom, respectively. Performing these analyses at a confidence level of 95% ( $\alpha = 0.05$ ) shows that values with P values less than 0.05 represent significant results. Significant P values are marked in bold in the ANOVA tables.

According to the ANOVA analyzes displayed in Tables 6–9, the most influential parameter was the depth of cut for energy consumption. Likewise, the depth of cut was the most effective parameter for electric current. The most effective parameter was feed rate for surface roughness and cutting speed for sound intensity level.

Table 6 shows that the most effective parameter for surface roughness is the feed rate with 87.42%, followed by cutting depth (1.94%) with minor contribution. Cutting speed has no significant effect. The square of the feed rate ( $f^2$ ) contributed to the surface roughness with a rate of 5.94%. It is clear that the feed rate is the main parameter theoretically, and the literature also supports this in the same direction [8, 18, 44]. The results achieved by Günay and Yücel [9] were consistent with the present work for a material with a hardness of 62 HRC, while the most effective parameter for a material with a hardness of 50 HRC was reported as the cutting speed. Likewise, Alok et al. [42] found the cutting speed to be the major parameter. As a result of another study, Mikolajczyk [25] modeled that the effect of

TABLE 5: Main effects plot for surface roughness, sound level, electric current, and energy consumption.

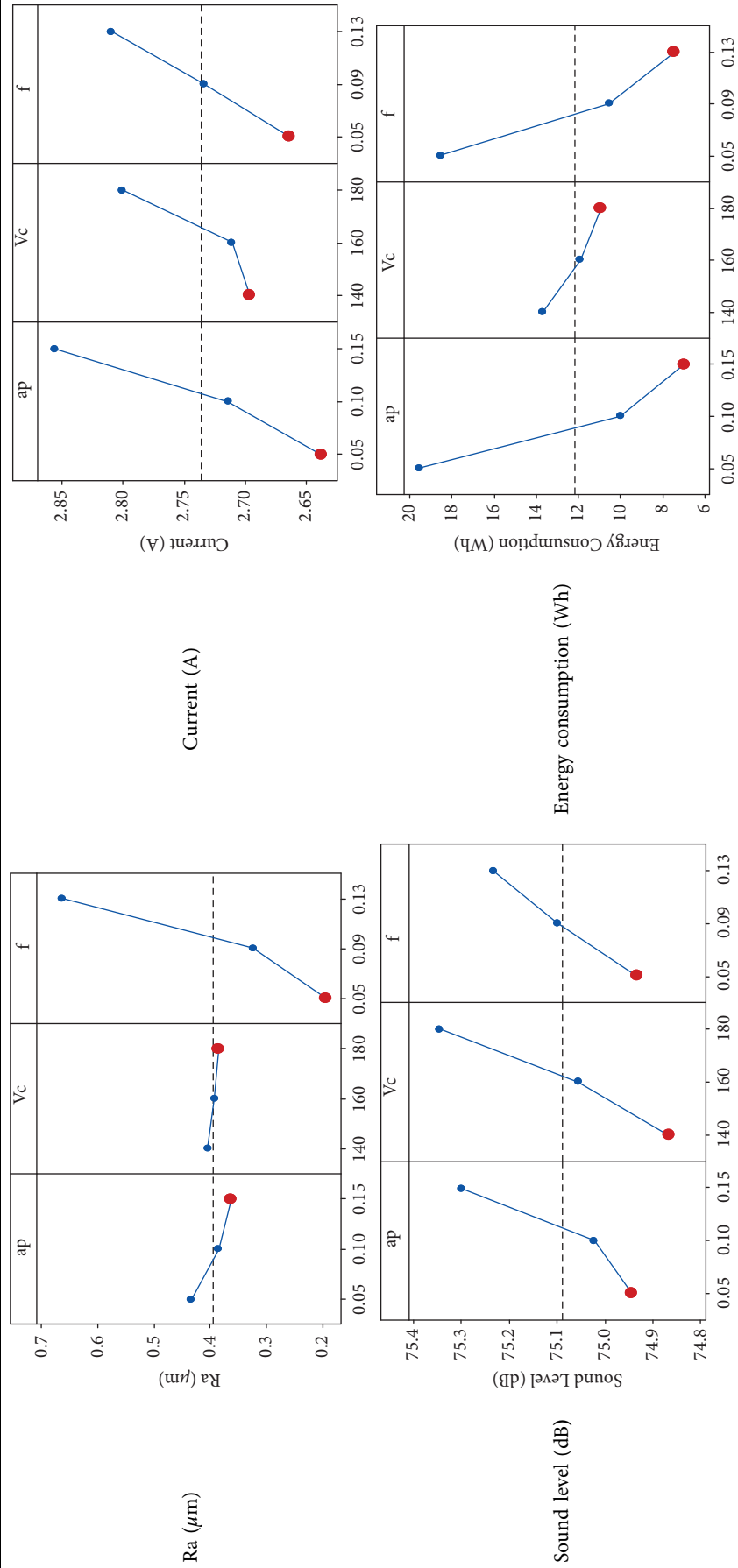


TABLE 6: Analysis of variance for surface roughness.

Source	DF	Adj SS	Adj MS	F value	P value	Contr. %
$a_p$	1	0.02205	0.022050	8.52	<b>0.010</b>	<b>1.94</b>
$V_c$	1	0.00161	0.001606	0.62	0.442	0.14
$F$	1	0.99405	0.994050	384.17	<b>≤0.001</b>	<b>87.42</b>
$a_p^2$	1	0.00098	0.000980	0.38	0.547	0.09
$V_c^2$	1	0.00005	0.000046	0.02	0.895	0.01
$f^2$	1	0.06756	0.067557	26.11	<b>≤0.001</b>	<b>5.94</b>
$a_p \times V_c$	1	0.00101	0.001008	0.39	0.541	0.09
$a_p \times f$	1	0.00563	0.005633	2.18	0.158	0.50
$V_c \times f$	1	0.00013	0.000133	0.05	0.823	0.01
Error	17	0.04399	0.002588	—	—	3.87
Total	26	1.13705	—	—	—	100.00

Significant  $P$  values are marked in bold.

TABLE 7: Analysis of variance for energy consumption.

Source	DF	Adj SS	Adj MS	F-value	P value	Contr. %
$a_p$	1	707.01	707.005	615.26	<b>≤0.001</b>	<b>46.15</b>
$V_c$	1	33.78	33.784	29.40	<b>≤0.001</b>	<b>2.21</b>
$F$	1	552.89	552.892	481.15	<b>≤0.001</b>	<b>36.09</b>
$a_p^2$	1	63.18	63.180	54.98	<b>≤0.001</b>	<b>4.12</b>
$V_c^2$	1	0.96	0.960	0.84	0.373	0.06
$f^2$	1	36.61	36.605	31.86	<b>≤0.001</b>	<b>2.39</b>
$a_p \times V_c$	1	7.74	7.744	6.74	<b>0.019</b>	<b>0.50</b>
$a_p \times f$	1	104.55	104.548	90.98	<b>≤0.001</b>	<b>6.82</b>
$V_c \times f$	1	5.64	5.644	4.91	<b>0.041</b>	<b>0.37</b>
Error	17	19.53	1.149	—	—	1.28
Total	26	1531.90	—	—	—	100.00

Significant  $P$  values are marked in bold.

TABLE 8: Analysis of variance for sound intensity level.

Source	DF	Adj SS	Adj MS	F value	P value	Contr. %
$a_p$	1	0.56889	0.56889	49.04	<b>≤0.001</b>	<b>24.88</b>
$V_c$	1	1.02722	1.02722	88.54	<b>≤0.001</b>	<b>44.92</b>
$F$	1	0.40500	0.40500	34.91	<b>≤0.001</b>	<b>17.71</b>
$a_p^2$	1	0.06000	0.06000	5.17	<b>0.036</b>	<b>2.62</b>
$V_c^2$	1	0.01500	0.01500	1.29	0.271	0.66
$f^2$	1	0.00167	0.00167	0.14	0.709	0.07
$a_p \times V_c$	1	0.00750	0.00750	0.65	0.432	0.33
$a_p \times f$	1	0.00333	0.00333	0.29	0.599	0.15
$V_c \times f$	1	0.00083	0.00083	0.07	0.792	0.04
Error	17	0.19722	0.01160	—	—	8.62
Total	26	2.28667	—	—	—	100.00

Significant  $P$  values are marked in bold.

MTCL has major influence on the surface roughness due to the nose radius.

The ANOVA in Table 8 shows that cutting speed, cutting depth, and feed rate were the most influential parameters for sound intensity levels with 44.92%, 24.88%, and 17.71%, respectively. Also, ( $a_p^2$ ) made a minor contribution. That is, the main parameter for the sound intensity level was the cutting speed. Similar to the results of the presented study, in some studies, the major parameter was obtained as the cutting speed [28].

According to Table 9, the major parameter on the electric current was the cutting depth with a rate of 52.20%. The other most effective parameters were the feed rate (23.08%)

TABLE 9: Analysis of variance for electric current.

Source	DF	Adj SS	Adj MS	F-value	P value	Contr. %
$a_p$	1	0.215606	0.215606	319.44	<b>≤0.001</b>	<b>52.20</b>
$V_c$	1	0.049089	0.049089	72.73	<b>≤0.001</b>	<b>11.89</b>
$F$	1	0.095339	0.095339	141.25	<b>≤0.001</b>	<b>23.08</b>
$a_p^2$	1	0.006446	0.006446	9.55	<b>0.007</b>	<b>1.56</b>
$V_c^2$	1	0.008563	0.008563	12.69	<b>0.002</b>	<b>2.07</b>
$f^2$	1	0.000046	0.000046	0.07	0.797	0.01
$a_p \times V_c$	1	0.009633	0.009633	14.27	<b>0.002</b>	<b>2.33</b>
$a_p \times f$	1	0.012033	0.012033	17.83	<b>0.001</b>	<b>2.91</b>
$V_c \times f$	1	0.004800	0.004800	7.11	<b>0.016</b>	<b>1.16</b>
Error	17	0.011474	0.000675	—	—	2.78
Total	26	0.413030	—	—	—	100.00

Significant  $P$  values are marked in bold.

and the cutting speed (11.89%). The parameters with minor influence were  $a_p \times f$ ,  $a_p \times V_c$ ,  $V_c^2$ ,  $a_p^2$ , and  $V_c \times f$ , respectively. In parallel, similar results were obtained with the study of Çakır [32]. According to the ANOVA results, they stated that the first and second most effective parameters are cutting speed and feed rate.

In Table 7, the most effective parameters on energy consumption were depth of cut (46.15%) and feed rate (36.09%). The study was found to be compatible with the literature [34]. Other effects were  $a_p \times f$  (% 6.82),  $a_p^2$  (%4.12),  $f^2$  (%2.39),  $V$  (%2.21),  $a_p \times V_c$ , and  $V_c \times f$ , respectively.

**3.3.3. 3D Surface Plots and Contour Graphs.** Figures 4–7 are 3D surface plots and contour graphs showing the relationship between cutting parameters and output variables.

From the 3D surface and contour plots in Figure 4, it is seen that surface roughness value increases with the increase of feed rate. Therefore, it is clear that low feed is advantageous for good surface quality. As the depth of cut increased, the surface roughness decreased somewhat. This is similar to some studies in the literature [28, 43]. The increased cutting speed slightly improved the surface quality. This is an expected result in this case [19]. Due to the closeness of the selected cutting speed parameters, there was no significant difference on the surface roughness values [29, 38].

The 3D surface and contour plots in Figure 5 show that the sound intensity level values increase with the increase of all cutting parameters. When these plots were analyzed, the highest rate of change was in cutting speed. Therefore, the cutting parameter that most affected sound intensity was cutting speed. The effects of depth of cut and feed rate were also significant, respectively [28]. The  $a_p \times V_c$  interaction was determined to be the most effective according to the contour plot.

From the 3D surface and contour plots in Figure 6, it is seen that the electric current values increase with the increase of all cutting parameters. It is seen that the most important parameter affecting the electric current value is the depth of cut [29]. According to the surface and contour graphics, it was determined that the  $a_p \times V_c$  interaction is important. In other words, the cutting speed was the second most effective parameter.

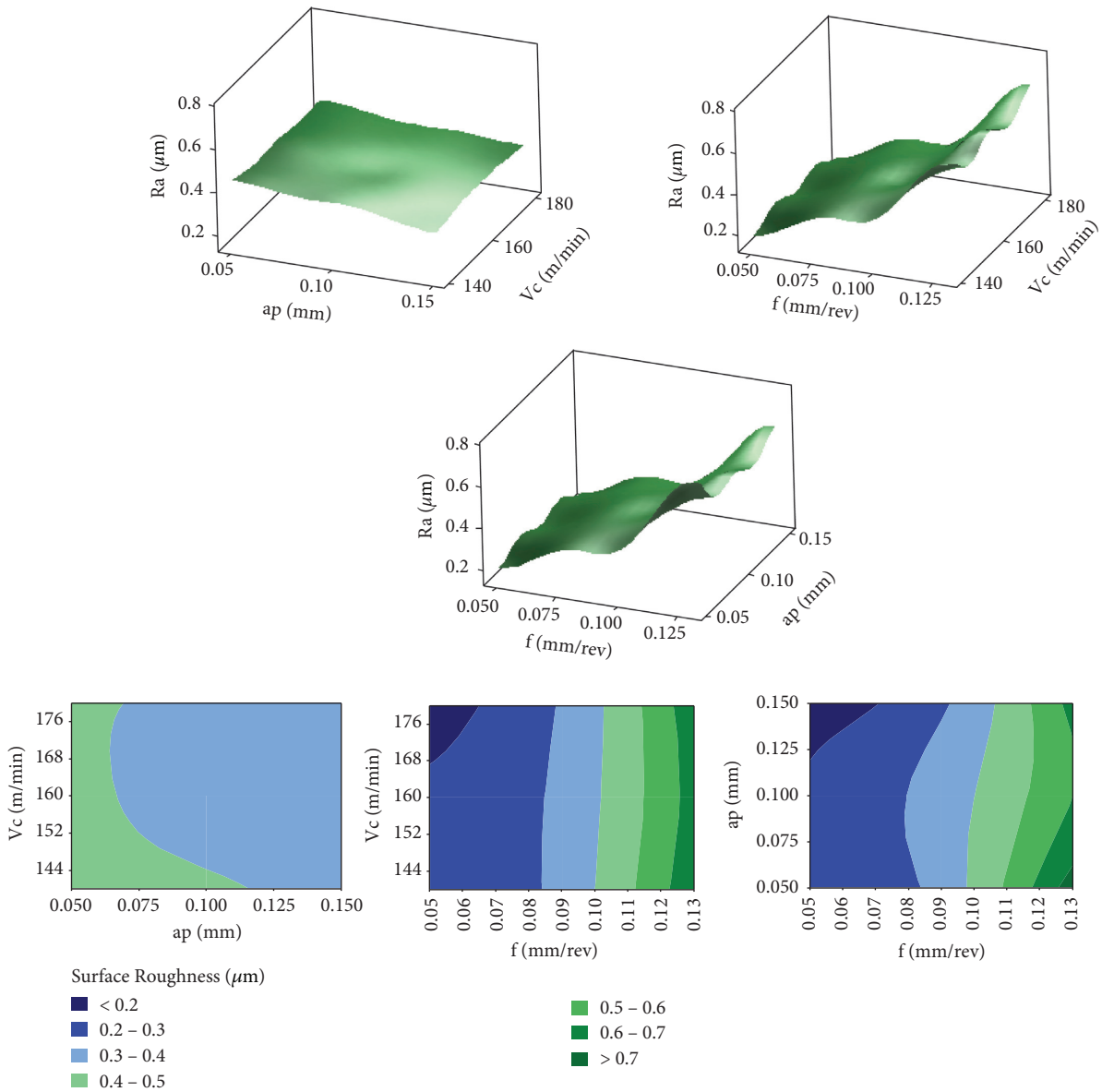


FIGURE 4: 3D surface plots and contour plots based on cutting parameters for surface roughness values.

Figure 7 demonstrates that energy consumption decreases with increased cutting parameters. The interaction of depth of cut and feed rate ( $a_p \times f$ ), depth of cut, and cutting speed ( $a_p * V_c$ ) showed the most important effect on surface graphics. Likewise, it was determined from the contour graphics that ( $a_p * f$ ) and ( $a_p * V_c$ ) are very important. It is understood from these graphs that the depth of cut is the most effective parameter.

**3.3.4. Optimization of Cutting Parameter.** Optimum levels are determined as the lowest values of the output parameters. The optimum input parameter levels and values are shown in Table 10, and the average optimum output values for each cutting parameter are indicated in bold fonts.

Optimum levels and values for surface roughness are high depth of cut (level 3, 0.15 mm), high cutting speed (level 3, 180 m/min), and most importantly low feed rate (level 1–0.05 mm/rev). Average surface roughness values for these optimum cutting parameters are  $0.36 \mu\text{m}$  for high depth of cut,  $0.39 \mu\text{m}$  for high cutting speed, and  $0.19 \mu\text{m}$  for low feed. In the studies carried out, the lowest surface roughness values were obtained at low feed rate and high cutting speeds [17, 18]. Some studies in the literature have shown that the surface roughness decreases slightly at higher depths of cut [24].

Low optimum cutting parameter levels (level 1:  $a_p = 0.05$ ,  $V_c = 140$  m/min, and  $f = 0.05$  mm/rev) were found for sound intensity level and electric current values, while high levels (level 3:  $a_p = 0.15$ ,  $V_c = 180$  m/min, and  $f = 0.15$  mm/rev) were found for energy consumption.

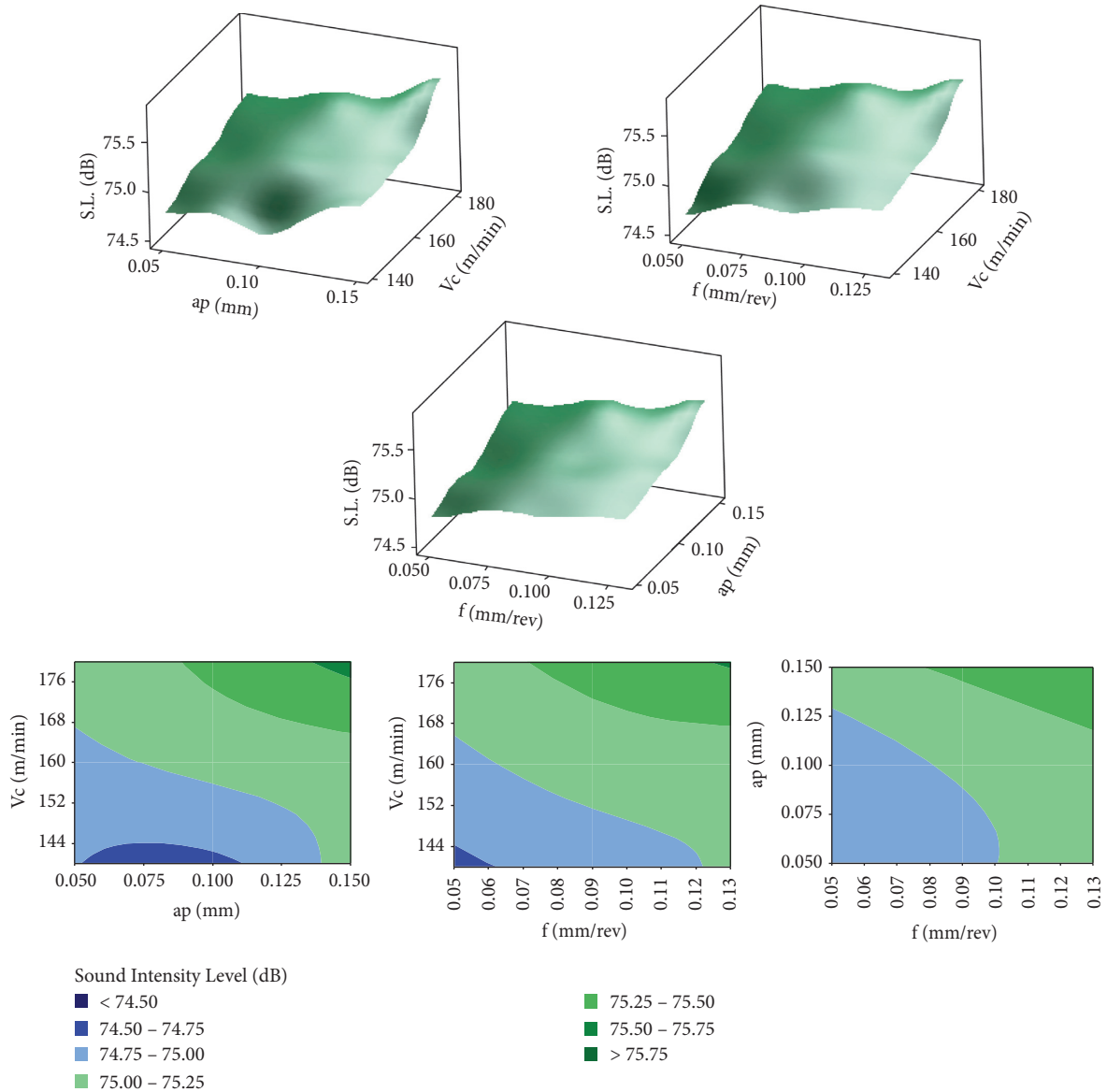


FIGURE 5: 3D surface plots and contour plots based on cutting parameters for sound intensity level.

**3.3.5. Establishment of Mathematical Models Using Regression Equations.** Multiple regression analysis was performed to understand the relationship between input (processing parameters or independent variables) and output parameters (response variables or dependent variables). A quadratic polynomial model was constructed for each dependent variable. To establish mathematical models, regression coefficient values were determined (for surface roughness, sound intensity level, electric current, and energy consumption). Independent variables and regression coefficients were calculated for the estimated dependent variables in equation (11).

$$\begin{aligned}
 Y &= \beta_0 + \beta_1 a_p + \beta_2 V_c + \beta_{11} a_p^2 \\
 &= \beta_{22} V_c^2 + \beta_{33} f^2 + \beta_{12} a_p * V_c + \beta_{13} a_p * f + \beta_{23} V_c * f,
 \end{aligned}
 \tag{11}$$

where  $Y$  (Ra, sound intensity level, electric current, and energy consumption) are dependent variables;  $a_p$  (depth of cut),  $V_c$  (cutting speed), and  $f$  (feed rate) are independent variables; and  $\beta_0, \beta_1, \beta_2, \dots, \beta_{33}$  are regression coefficients.

The  $R^2$  determination coefficient was calculated for each dependent variable from equation (12).

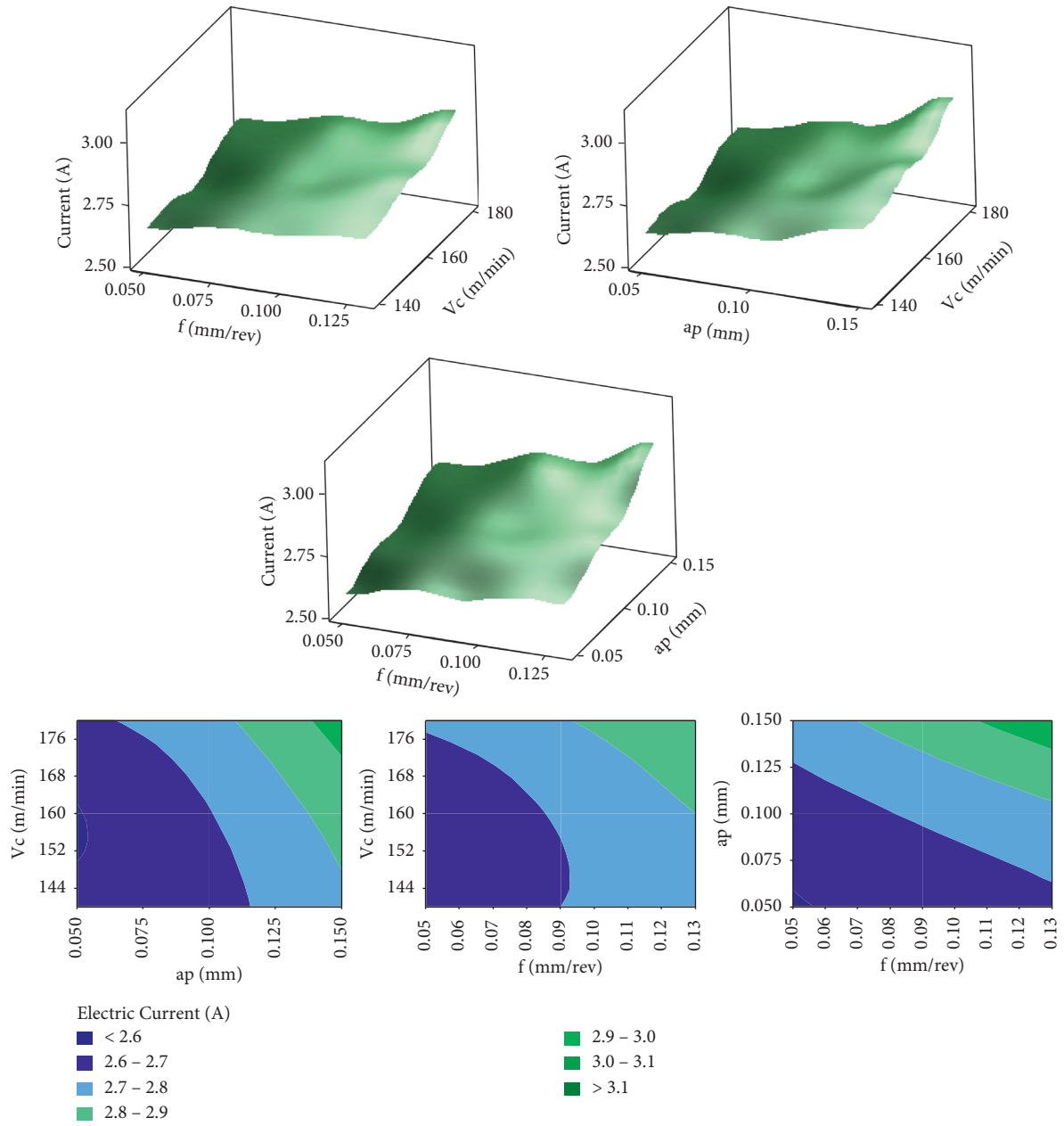


FIGURE 6: 3D surface plots and contour plots based on cutting parameters for electric current value.

$$R^2 = 1 - \frac{SS_{residual}}{SS_{model} + SS_{residual}}, \quad (12)$$

The regression formulas and determination coefficients (equations (13)–(16)) are as follows:

where  $SS_{residual}$  is sum of squares residual and  $SS_{model}$  is sum of squares model.

$$\begin{aligned} \text{surface roughness} = & 0.81 - 2.21 * a_p - 0.004 * V_c - 5.65 * f + 5.11 * a_p^2 \\ & + 0.000007 * V_c^2 + 66.3 * f^2 + 0.0092 * a_p * V_c - 10.83 * a_p * f + 0.0042 * V_c * f, \end{aligned}$$

$$R^2 = 96.13\%,$$

$$R^2 (\text{adj}) = 94.08\%,$$

(13)

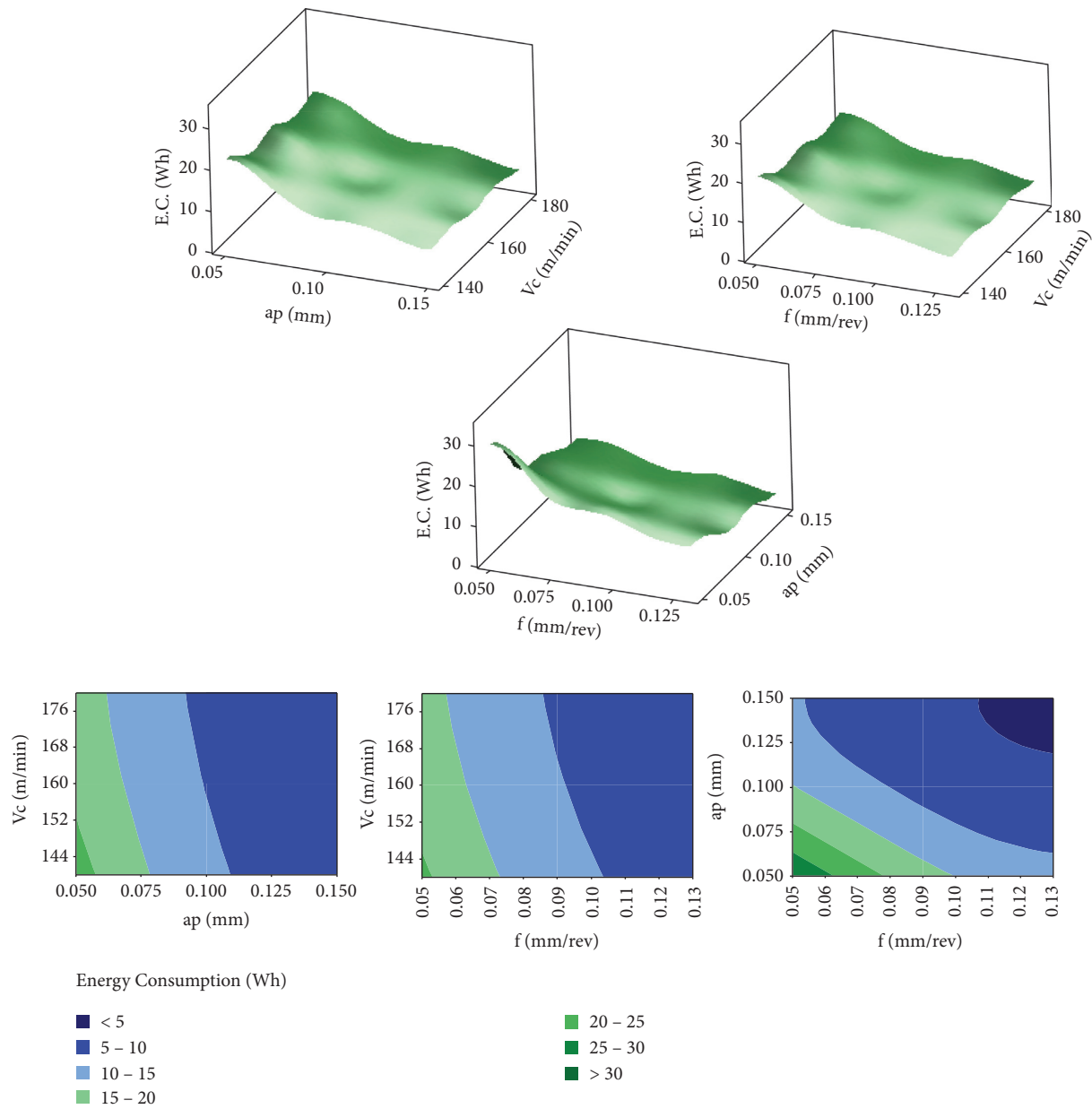


FIGURE 7: 3D surface plots and contour plots based on cutting parameters for energy consumption value.

TABLE 10: Optimum cutting parameters level (D) and value (V) for surface roughness (Ra), electric current, sound intensity level, and energy consumption.

	Ra ( $\mu\text{m}$ )			Sound level (dB)			Electric current (A)			Energy consumption (kWh)		
	$a_p$ (mm)	$V_c$ (m/min)	$f$ (mm/rev)	$a_p$ (mm)	$V_c$ (m/min)	$f$ (mm/rev)	$a_p$ (mm)	$V_c$ (m/min)	$f$ (mm/rev)	$a_p$ (mm)	$V_c$ (m/min)	$f$ (mm/rev)
1	0.43	0.40	<b>0.19</b>	<b>74.94</b>	<b>74.87</b>	<b>74.93</b>	<b>2.64</b>	<b>2.70</b>	<b>2.66</b>	19.53	13.68	18.54
2	0.39	0.39	0.32	75.02	75.06	75.10	2.71	2.71	2.73	10.01	11.91	10.53
3	<b>0.36</b>	<b>0.38</b>	0.66	75.30	75.34	75.23	2.86	2.80	2.81	<b>6.99</b>	<b>10.94</b>	<b>7.46</b>
<b>D</b>	<b>3</b>	<b>3</b>	<b>1</b>	<b>1</b>	<b>1</b>	<b>1</b>	<b>1</b>	<b>1</b>	<b>1</b>	<b>3</b>	<b>3</b>	<b>3</b>
<b>V</b>	<b>0.15</b>	<b>180</b>	<b>0.05</b>	<b>0.05</b>	<b>140</b>	<b>0.05</b>	<b>0.05</b>	<b>140</b>	<b>0.05</b>	<b>0.15</b>	<b>180</b>	<b>0.13</b>

The bold values represent optimum values for each cutting parameter. D: level of optimum input parameters; V: optimum input values.

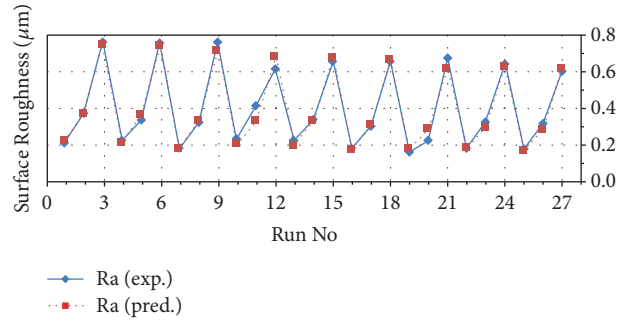


FIGURE 8: Comparison between predicted and measured values for surface roughness.

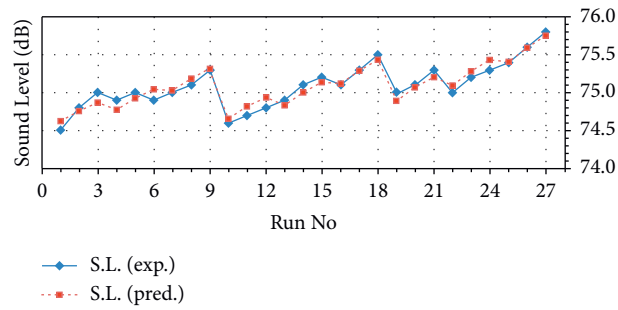


FIGURE 9: Comparison between predicted and measured values for sound intensity level.

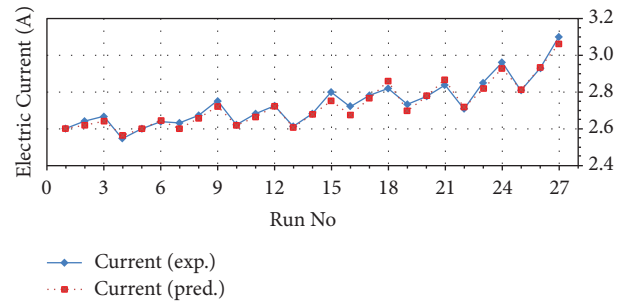


FIGURE 10: Comparison between predicted and measured values for electric current.

$$\begin{aligned}
 \text{sound intensity} &= 76.54 - 9.19 * a_p - 0.0315 * V_c + 3.12 * f + 40.0 * a_p^2 \\
 &\quad + 0.000125 * V_p^2 - 10.4 * f^2 + 0.0250 * a_p * V_c + 8.3 * a_p * f + 0.0104 * V_c * f, \\
 R^2 &= 91.38\%, \\
 R^2(\text{adj}) &= 86.81\%,
 \end{aligned}
 \tag{14}$$

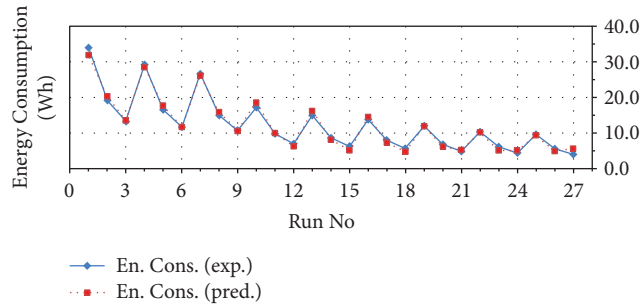


FIGURE 11: Comparison between predicted and measured values for energy consumption.

$$\begin{aligned}
 \text{machine current} &= 5.406 - 6.39 * a_p - 0.032694 * V_c - 4.08 * f + 13.11 * a_p^2 \\
 &\quad - 0.000094 * V_c^2 + 1.74 * f^2 + 0.02833 * a_p * V_c + 15.83 * a_p * f + 0.025 * V_c * f, \\
 R^2 &= 97.22\%, \\
 R^2(\text{adj}) &= 95.75\%,
 \end{aligned} \tag{15}$$

$$\begin{aligned}
 \text{energy consumption} &= 133.6 - 646.3 * a_p - 0.546 * V_c - 701.2 * f + 1298 * a_p^2 \\
 &\quad + 0.00100 * V_c^2 + 1544 * f^2 + 0.803 * a_p * V_c + 1476 * a_p * f + 0.857 * V_c * f, \\
 R^2 &= 98.72\%, \\
 R^2(\text{adj}) &= 98.05\%.
 \end{aligned} \tag{16}$$

3.3.6. *Comparison Tests.* Figures 8–11 express the comparisons of the experimental results and mathematical model results. The experimental results are indicated in blue and the mathematical (prediction) models in red. As seen in the figures, these values are very close to each other and have no significant difference between them. High  $R^2$  values indicate that the mathematical model values will produce results that are similar to the experimental data.

## 4. Conclusions

In this study, hard turning of AISI H11 hot work tool steel was carried out by using a PVD-coated carbide tool and coolant. The relationship between input parameters ( $a_p$ ,  $V_c$ , and  $f$ ) and output variables (surface roughness, sound intensity level, electric current, and energy consumption) was statistically interpreted using the RSM.

- (1) According to the statistical analysis results (ANOVA), the major influence for surface roughness (Ra) was feed rate by 88.62%, and the product of feed rate ( $f^2$ ) followed a contribution by 5.94%. According to the surface and contour plots, as well as the main effect plots, the relationship of feed rate on surface roughness was clear. Considering the optimum cutting parameter values, the surface roughness values increased from 0.19 to 0.68 (approximately 350%) with the increase in the feed rate. Thus, increasing the feed rate deteriorated the surface quality. The effect of the depth of cutting is minimal (1.94%), and it was

determined that cutting speed had no effect on Ra. Surface roughness decreased with low feed rate, high cutting speed, and high depth of cut. Mathematical modeling was created by finding a determination value of 96.13% for Ra. So, there was no significant difference between the actual results and the predicted mathematical model.

- (2) According to the statistical analysis results (ANOVA), the most effective parameters for sound intensity level were cutting speed (44.92%), depth of cut (24.88%), and feed rate (17.71%), respectively. From the surface, contour, and main effect graphic analyses, it was determined that the sound intensity level increased with the increase of cutting parameters. Since the surface roughness values of all experiments were low, an excessive sound intensity level did not occur (74.5–75.8 dB). It was analyzed that there was a significant increase in the sound intensity of the machine with increasing cutting speeds. Consistent results were obtained in the literature studies.  $R^2$  for sound intensity level is 91.38%. Similar results were obtained when the experimental and predictive mathematical models were compared. In addition, it is important to make such measurements in terms of the health of the employees; sound intensity level measurement is a very practical and inexpensive method and can be used successfully in future studies.
- (3) The major parameter for electric current and energy consumption was depth of cut (52.20% and 46.15%,

respectively). Another important parameter for both response parameters was feed rate (23.08% and 36.09%, respectively). Cutting speed was an effective parameter by 11.89% for electric current. Also, for electric current ( $a_p * f$ ) ( $V_c * f$ ) interactions and cutting speed squared ( $V_c^2$ ) had little effect. The  $a_p * f$  interaction and their squares ( $a_p^2$ ,  $V_c^2$ ) had minor effect on energy consumption. It is an expected result that energy consumption decreases with increasing cutting parameters. Because the studies and theoretical calculations proved this situation, real and mathematical model results of electric current ( $R^2=97.22\%$ ) and energy consumption ( $R^2=98.72\%$ ) are almost similar.

- (4) While there is a direct proportionality between the sound intensity level and the electrical current values, there is an inverse relationship between them and the energy consumption, because, for the calculation of energy consumption, it is necessary to remove an equal amount of chip thickness from the workpiece. Therefore, longer machining time is required for lower depth of cut. Likewise, the amount of energy consumption will increase as the machining time will be longer with low cutting speed and low feed rate.
- (5) Surface roughness (Ra), sound intensity level, and electric current values increased with increasing feed rates. On the contrary, energy consumption decreased with increasing feed rates. Ra decreased with increasing depth of cut. Likewise, Ra decreased with increasing cutting speed, albeit limited. In addition, as depth of cut and cutting speed increased, sound intensity levels and electric current values increased. On the other hand, as these values increased, energy consumption values decreased. In other words, the increase of all cutting parameters decreased the total machining time. Thus, energy consumption has also decreased.
- (6) According to the test results, the average surface roughness values are in a low range (0.16–0.76  $\mu\text{m}$ ). Therefore, for hard turning, it has been observed that PVD-coated carbide tool can be an alternative to expensive tools at 50 HRC hardness. In addition, we have provided great advantages in terms of manufacturing, as we have achieved surface roughness in grinding quality in the hard turning processes we have carried out (the average of 27 test results was obtained as 0.4  $\mu\text{m}$ ).
- (7) With proper energy savings, the environment can be protected at the maximum level. Energy consumption should be minimized to save energy. In this vein, machining time can be shortened by increasing the cutting parameter values to optimum levels to reduce energy consumption. In addition to low energy consumption, the material must be processed with a good surface quality. A low feed rate is required for a good surface quality. Such studies should be accelerated for a sustainable and healthy life in the future.

## Nomenclature

AISI:	American Iron and Steel Institute
CNC:	Computer numerical control
PVD:	Physical vapor deposition
CBN:	Cubic boron nitride
HRC:	Rockwell hardness
RSM:	Response surface methodology
ANOVA:	Analysis of variance
2D:	Two-dimensional
3D:	Three-dimensional
DCMT:	Cutting insert size
MS:	Mean of squares
SS:	Sum of squares
DF:	Degree of freedom
P:	Probability of significance
F:	Variance ratio
Exp:	Experimental
Pred:	Predicted
t:	Machining time, s
T:	Total machining time, s
N:	Spindle speed, rpm
D:	Diameter, mm
L:	Processing length, mm
f:	Feed rate, mm/rev
$V_c$ :	Cutting speed, m/min
$a_p$ :	Depth of cut, mm
$a_{pmax}$ :	Maximum depth of cut, mm
r:	Nose radius, mm
I:	Current, A
V:	Voltage, V
Ra:	Average surface roughness, $\mu\text{m}$
S.L.:	Sound intensity level, Db
Y:	Response parameter
$\Phi$ :	Phase angle
$\emptyset$ :	Output parameter function.

## Data Availability

All data generated or analyzed during this study are included in this article.

## Conflicts of Interest

The authors declare no conflicts of interest.

## References

- [1] P. L. Khan and S. V. Bhivane, "Experimental analysis and investigation of machining parameters in finish hard turning of AISI 4340 steel," *Procedia Manufacturing*, vol. 20, pp. 265–270, 2018.
- [2] J. P. Davim and L. Figueira, "Machinability evaluation in hard turning of cold work tool steel (D2) with ceramic tools using statistical techniques," *Materials & Design*, vol. 28, no. 4, pp. 1186–1191, 2007.
- [3] A. Anand, A. K. Behera, and S. R. Das, "An overview on economic machining of hardened steels by hard turning and its process variables," *Manufacturing Review*, vol. 6, no. 4, pp. 4–9, 2019.

- [4] N. A. Özbek, "Optimization of flank wear and surface quality in the turning of 1.2343 tool steel using carbide tools coated via different methods," *Surface Topography: Metrology and Properties*, vol. 9, no. 2, Article ID 025028, 2021.
- [5] S. Benlahmidi, H. Aouici, F. Boutaghane, A. Khellaf, B. Fnides, and M. A. Yallese, "Design optimization of cutting parameters when turning hardened AISI H11 steel (50 HRC) with CBN7020 tools," *International Journal of Advanced Manufacturing Technology*, vol. 89, no. 1-4, pp. 803–820, 2017.
- [6] R. Bhatti and R. Singh, "Optimization of cutting parameters on AISI H11 steel using multi-coated carbide tool by taguchi method," *International Journal of Current Engineering and Technology*, vol. 5, no. 4, pp. 2418–2424, 2015.
- [7] F. Karaaslan and A. Şahinoğlu, "Determination of ideal cutting conditions for maximum surface quality and minimum power consumption during hard turning of AISI 4140 steel using TOPSIS method based on fuzzy distance," *Arabian Journal for Science and Engineering*, vol. 45, no. 11, pp. 9145–9157, 2020.
- [8] A. Agrawal, S. Goel, W. B. Rashid, and M. Price, "Prediction of surface roughness during hard turning of AISI 4340 steel (69 HRC)," *Applied Soft Computing*, vol. 30, pp. 279–286, 2015.
- [9] M. Günay and E. Yücel, "Application of taguchi method for determining optimum surface roughness in turning of high-alloy white cast iron," *Measurement*, vol. 46, no. 2, pp. 913–919, 2013.
- [10] A. Das, S. K. Patel, T. K. Hotta, and B. B. Biswal, "Statistical analysis of different machining characteristics of EN-24 alloy steel during dry hard turning with multilayer coated cermet inserts," *Measurement*, vol. 134, pp. 123–141, 2019.
- [11] A. Panda, S. Ranjan Das, and D. Dhupal, "Machinability investigation of HSLA steel in hard turning with coated ceramic tool: assessment, modeling, optimization and economic aspects," *Journal of Advanced Manufacturing Systems*, vol. 18, no. 4, pp. 625–655, 2019.
- [12] F. M. Aneiro, R. T. Coelho, and L. C. Brandão, "Turning hardened steel using coated carbide at high cutting speeds," *Journal of the Brazilian Society of Mechanical Sciences and Engineering*, vol. 30, no. 2, pp. 104–109, 2008.
- [13] R. Suresh, A. G. Joshi, and M. Manjiaiah, "Experimental Investigation on tool wear in AISI H13 die steel turning using RSM and ANN methods," *Arabian Journal for Science and Engineering*, vol. 46, no. 3, pp. 2311–2325, 2021.
- [14] A. Chavan and V. Sargade, "Surface integrity of AISI 52100 Steel during hard turning in different near-dry environments," *Advances in Materials Science and Engineering*, vol. 2020, Article ID 4256308, 13 pages, 2020.
- [15] R. Tiwari, D. Das, A. Kumar Sahoo, R. Kumar, R. Kumar Das, and B. Chandra Routara, "Experimental investigation on surface roughness and tool wear in hard turning JIS S45C steel," *Materials Today: Proceedings*, vol. 5, no. 11, pp. 24535–24540, 2018.
- [16] A. Alok and M. Das, "Multi-objective optimization of cutting parameters during sustainable dry hard turning of AISI 52100 steel with newly develop HSN2-coated carbide insert," *Measurement*, vol. 133, pp. 288–302, 2019.
- [17] S. Sahu and B. B. Choudhury, "Optimization of surface roughness using taguchi methodology & prediction of tool wear in hard turning tools," *Materials Today: Proceedings*, vol. 2, no. 4-5, pp. 2615–2623, 2015.
- [18] H. Aouici, B. Fnides, M. Elbah, S. Benlahmidi, H. Bensouilah, and M. A. Yallese, "Surface roughness evaluation of various cutting materials in hard turning of AISI H11," *International Journal of Industrial Engineering Computations*, vol. 7, no. 2, pp. 339–352, 2016.
- [19] A. Şahinoğlu and M. Rafiqhi, "Investigation of vibration, sound intensity, machine current and surface roughness values of AISI 4140 during machining on the lathe," *Arabian Journal for Science and Engineering*, vol. 45, no. 2, pp. 765–778, 2020.
- [20] A. Singh and M. K. Sinha, "Multi-response optimization during dry turning of bio-implant steel (AISI 316L) using coated carbide inserts," *Arabian Journal for Science and Engineering*, vol. 45, no. 11, pp. 9397–9411, 2020.
- [21] A. Awale and K. Inamdar, "Multi-objective optimization of high-speed turning parameters for hardened AISI S7 tool steel using grey relational analysis," *Journal of the Brazilian Society of Mechanical Sciences and Engineering*, vol. 42, no. 7, pp. 1–17, 2020.
- [22] M. Nouioua, M. A. Yallese, R. Khettabi, S. Belhadi, M. L. Bouhalais, and F. Girardin, "Investigation of the performance of the MQL, dry, and wet turning by response surface methodology (RSM) and artificial neural network (ANN)," *International Journal of Advanced Manufacturing Technology*, vol. 93, no. 5-8, pp. 2485–2504, 2017.
- [23] P. Umamaheswarrao, D. R. Raju, K. Suman, and B. R. Sankar, "Multi objective optimization of process parameters for hard turning of AISI 52100 steel using Hybrid GRA-PCA," *Procedia Computer Science*, vol. 133, pp. 703–710, 2018.
- [24] A. Panda, S. R. Das, and D. Dhupal, "Surface roughness analysis for economical feasibility study of coated ceramic tool in hard turning operation," *Process Integration and Optimization for Sustainability*, vol. 1, no. 4, pp. 237–249, 2017.
- [25] T. Mikolajczyk, "Modeling of minimal thickness cutting layer influence on surface roughness in turning," *Applied Mechanics and Materials*, vol. 656, pp. 262–269, 2014.
- [26] T. Mikolajczyk, H. Latos, D. Y. Pimenov, T. Paczkowski, M. K. Gupta, and G. Krolczyk, "Influence of the main cutting edge angle value on minimum uncut chip thickness during turning of C45 steel," *Journal of Manufacturing Processes*, vol. 57, pp. 354–362, 2020.
- [27] Y. Deshpande, A. Andhare, and N. K. Sahu, "Estimation of surface roughness using cutting parameters, force, sound, and vibration in turning of Inconel 718," *Journal of the Brazilian Society of Mechanical Sciences and Engineering*, vol. 39, no. 12, pp. 5087–5096, 2017.
- [28] A. Şahinoğlu and M. Rafiqhi, "Machinability of hardened AISI S1 cold work tool steel using cubic boron nitride," *Scientia Iranica*, pp. 1–28, 2021.
- [29] A. K. Cakir, "Analysis of surface roughness, sound level and machine current in the turning of hardened AISI S1 steel," *Transactions of the Indian Institute of Metals*, vol. 74, no. 3, pp. 691–703, 2021.
- [30] D. Rastorguev and A. Sevastyanov, "Diagnostics of chip formation and surface quality by parameters of the main drive current in the hard turning," *Materials Today: Proceedings*, vol. 19, pp. 1845–1851, 2019.
- [31] P. S. Bilga, S. Singh, and R. Kumar, "Optimization of energy consumption response parameters for turning operation using Taguchi method," *Journal of Cleaner Production*, vol. 137, pp. 1406–1417, 2016.
- [32] M. E. Korkmaz and M. Günay, "Finite element modelling of cutting forces and power consumption in turning of AISI 420 martensitic stainless steel," *Arabian Journal for Science and Engineering*, vol. 43, no. 9, pp. 4863–4870, 2018.
- [33] C. Camposeco-Negrete and J. de Dios Calderón-Nájera, "Sustainable machining as a mean of reducing the

- environmental impacts related to the energy consumption of the machine tool: a case study of AISI 1045 steel machining,” *International Journal of Advanced Manufacturing Technology*, vol. 102, no. 1-4, pp. 27–41, 2019.
- [34] S. Velchev, I. Kolev, K. Ivanov, and S. Gechevski, “Empirical models for specific energy consumption and optimization of cutting parameters for minimizing energy consumption during turning,” *Journal of Cleaner Production*, vol. 80, pp. 139–149, 2014.
- [35] B. Öztürk and F. Kara, “Calculation and estimation of surface roughness and energy consumption in milling of 6061 alloy,” *Advances in Materials Science and Engineering*, vol. 2020, Article ID 5687951, 12 pages, 2020.
- [36] E. A. Ayyıldız, M. Ayyıldız, and F. Kara, “Optimization of surface roughness in drilling medium-density fiberboard with a parallel robot,” *Advances in Materials Science and Engineering*, vol. 2021, Article ID 6658968, 8 pages, 2021.
- [37] M. Kuntoğlu, O. Acar, M. K. Gupta et al., “Parametric optimization for cutting forces and material removal rate in the turning of AISI 5140,” *Machines*, vol. 9, no. 5, p. 90, 2021.
- [38] K. V. Subbaiah, C. Raju, and C. Suresh, “Parametric analysis and optimization of hard turning at different levels of hardness using wiper ceramic insert,” *Measurement*, vol. 158, Article ID 107712, 2020.
- [39] F. Kara, “Taguchi optimization of surface roughness and flank wear during the turning of DIN 1.2344 tool steel,” *Mater Test*, vol. 59, no. 10, pp. 903–908, 2017.
- [40] M. Kuntoğlu, A. Aslan, D. Y. Pimenov, K. Giasin, T. Mikolajczyk, and S. Sharma, “Modeling of cutting parameters and tool geometry for multi-criteria optimization of surface roughness and vibration via response surface methodology in turning of AISI 5140 steel,” *Materials*, vol. 13, no. 19, p. 4242, 2020.
- [41] Birleşik metal, “Birleşik metal and special alloys,” 2012, <https://www.birlesikmetal.eu/Materials/12343>.
- [42] A. Alok, A. Kumar, and M. Das, “Hard Turning with a new HSN 2 -coated carbide insert and optimization of process parameter,” *Transactions of the Indian Institute of Metals*, vol. 74, pp. 1577–1591, 2021.
- [43] M. Rafighi, M. Özdemir, S. Al Shehabi, and M. T. Kaya, “Sustainable hard turning of high chromium AISI D2 tool steel using CBN and ceramic inserts,” *Transactions of the Indian Institute of Metals*, vol. 74, 2021.
- [44] A. Khellaf, H. Aouici, S. Smaiah, S. Boutabba, M. A. Yallese, and M. Elbah, “Comparative assessment of two ceramic cutting tools on surface roughness in hard turning of AISI H11 steel: including 2D and 3D surface topography,” *International Journal of Advanced Manufacturing Technology*, vol. 89, no. 1–4, pp. 333–354, 2017.